

See discussions, stats, and author profiles for this publication at: <https://www.researchgate.net/publication/225306076>

Picosecond Pulse Radiolysis Study of Highly Concentrated Nitric Acid Solutions: Formation Mechanism of $\text{NO}_3 \cdot$ Radical

ARTICLE in THE JOURNAL OF PHYSICAL CHEMISTRY A · JUNE 2012

Impact Factor: 2.69 · DOI: 10.1021/jp304429f · Source: PubMed

CITATIONS

9

READS

61

5 AUTHORS, INCLUDING:



[Anna Balcerzyk](#)

Université Paris-Sud 11

8 PUBLICATIONS 61 CITATIONS

SEE PROFILE



[Abdel Karim El Omar](#)

Lebanese University

11 PUBLICATIONS 110 CITATIONS

SEE PROFILE



[Uli Schmidhammer](#)

Université Paris-Sud 11

54 PUBLICATIONS 516 CITATIONS

SEE PROFILE



[Mehran Mostafavi](#)

Université Paris-Sud 11

162 PUBLICATIONS 2,907 CITATIONS

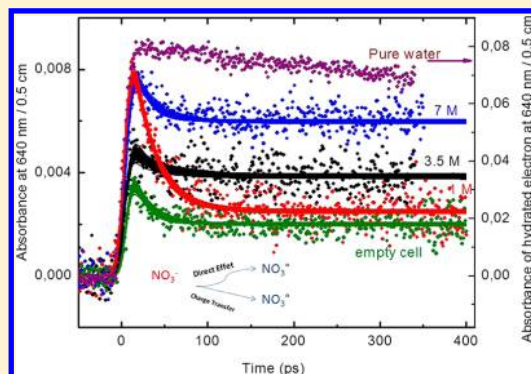
SEE PROFILE

Picosecond Pulse Radiolysis Study of Highly Concentrated Nitric Acid Solutions: Formation Mechanism of NO_3^\bullet Radical

Anna Balcerzyk, Abdel Karim El Omar, Uli Schmidhammer, Pascal Pernot, and Mehran Mostafavi*

Laboratoire de Chimie Physique/ELYSE, CNRS/Université Paris-Sud, Faculté des Sciences d'Orsay, Bât. 349, 91405 Orsay Cedex, France

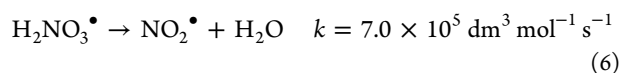
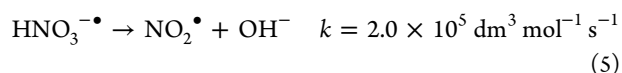
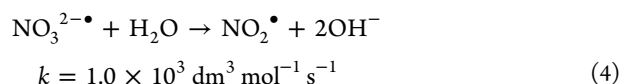
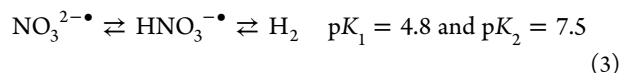
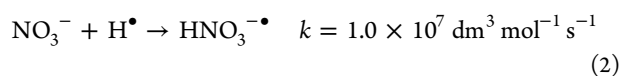
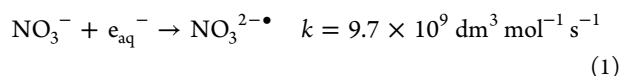
ABSTRACT: The formation of nitrate radical, NO_3^\bullet , is observed for the first time directly by picosecond pulse radiolysis of highly concentrated nitric acid solutions. The experimental yield of NO_3^\bullet ionization is deduced from the pulse–probe transient absorption measurements in the visible region where this radical absorbs. On the basis of the value of the extinction coefficient of nitrate radical at 640 nm equal to 1300 M cm^{-1} , the experimental yield of NO_3^\bullet at 20 ps is found to be around 0.36×10^{-7} , 1.33×10^{-7} , and $2.85 \times 10^{-7} \text{ mol J}^{-1}$ for 1, 3.5, and 7 M nitric acid solutions, respectively. Relative to the dose absorbed by nitric acid by the direct effect, we find an unexpected high formation yield of the nitrate radical within the electron pulse. Therefore, we suggest that the trapping of the positive hole, $\text{H}_2\text{O}^{\bullet+}$, by NO_3^- also contributes to the formation of NO_3^\bullet within the electron pulse. Moreover, after the pulse and within 4 ns, the beginning of the reaction of OH^\bullet radical with undissociated nitric acid is observed for the most concentrated nitric acid solution.



■ INTRODUCTION

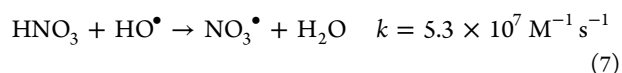
Radiolysis of nitric acid has been a matter of research since the middle of the last century. For the first time, the radiolysis study of nitric acid was performed in the 1950s at the Oak Ridge National Laboratory.¹ From the practical point of view, in nuclear technology, highly concentrated solutions of nitric acid are used for waste fuel reprocessing, and such solutions are considered to be a preferential medium even for the future processing of spent nuclear fuel with generation IV reactors. In such a case, aside from the indirect action of ionizing radiation, the direct radiation effect in concentrated solution has to be considered. The chemistry of nitric acid is very important for understanding the radiolysis of aqueous solutions containing nitrate ion, which is a very efficient scavenger of the hydrated electron, as well as the presolvated electron.² Moreover, the nitrate radical dominates the complex chemistry of the nighttime atmosphere, and the mechanism of its production and reactivity in atmosphere is also under investigation.³

When diluted solutions of nitric acid are irradiated, the reduction of the NO_3^- anion by the solvated electron and hydrogen atom takes place. As a result of NO_3^- reduction, NO_2^\bullet radicals are formed. NO_2^\bullet radical formation takes place via transient intermediates such as $\text{NO}_3^{2-\bullet}$, $\text{HNO}_3^{\bullet-}$, and $\text{H}_2\text{NO}_3^\bullet$ according to the following reactions:^{4–7}



The product of the radiolysis of diluted solutions, NO_2^\bullet radical, undergoes a reaction of recombination giving N_2O_4 , and from its decay, HNO_2 and HNO_3 are formed.

It is reported that the OH^\bullet radical reacts only with undissociated nitric acid by the following reaction:⁸



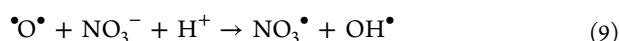
The amount of undissociated groups in diluted solution is very low, and the reaction is slow. This is why the formation of NO_3^\bullet radical through reaction 7 in dilute solutions is negligible.

By using microsecond pulse radiolysis, the mechanism of NO_3^\bullet radical formation in concentrated solutions was first announced to proceed according to the following reactions:^{9,10}

Received: May 7, 2012

Revised: June 12, 2012

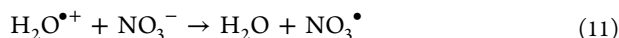
Published: June 13, 2012



Later, nanosecond pulse radiolysis of 3 and 6 M NaNO_3 was performed by Katsumura et al.,⁸ and by observing the formation of NO_3^\bullet within the nanosecond electron pulse, a second mechanism was proposed implying the direct ionization of nitrate ions as follows:



The possibility of the scavenging of the hole (the precursor of OH^\bullet radical) by NO_3^- was also evoked without any conclusion on its occurrence.⁸



The hole in pure water is delocalized on a few water molecules, but in order to simplify, we use here the notation $\text{H}_2\text{O}^{\bullet+}$ for the hole in water.¹¹ In pure water, the hole reacts very fast to form OH^\bullet radical as follows:



If we assume the above reactions 1–7 are true, we find that the radical NO_3^\bullet cannot be formed on the picosecond range, except by direct effect in highly concentrated nitric acid or by hole trapping. In fact, reaction 7 is not controlled by diffusion, and even with a few molar nitric acid, the radical NO_3^\bullet can be observed only at longer time than a few nanoseconds, as it was observed by Katsumura et al.⁸

On the basis of the experiments with highly concentrated Br^- and Cl^- solutions,^{12,13} we performed the picosecond pulse radiolysis studies of concentrated solutions of nitric acid. This time resolution is helpful to distinguish between different possibilities of NO_3^\bullet formation in irradiated highly concentrated nitric acid. In fact, four different mechanisms could be involved in the formation of NO_3^\bullet radical: (i) direct effect through reaction 10; (ii) hole scavenging through reaction 11; (iii) via NO_3^- dissociation through reactions 8 and 9; and (iv) reaction of OH^\bullet with undissociated HNO_3 by reaction 7. With varying concentrations of nitric acid (1, 3.5, and 7 M) the yield of NO_3^\bullet formation is examined by picosecond pulse radiolysis measurements, and the occurrence of the above mechanisms of NO_3^\bullet formation is discussed.

EXPERIMENTAL SECTION

The transient absorption pulse–probe setup is based on the laser–electron intrinsic synchronization resulting from the laser-triggered photocathode¹⁴ and was detailed elsewhere.^{13,15} Shortly, the main part of a femtosecond Ti:Sapphire laser output is frequency tripled and used to produce the electron pulse that is accelerated by the RF fields. A part of the laser source is split off to generate the optical probe pulse that can be delayed relative to the electron bunch by a mechanical translation stage. About 1 μJ of the laser source was focused into a 6 mm thick CaF_2 disk to generate a supercontinuum used as the optical probe. A reference signal is split off from the broadband probe before the fused silica optical flow cell (FSOFC). Probe and reference beams were each coupled into an optical fiber, transmitted to a spectrometer, and dispersed onto a CCD. The combination of the broadband probe and the multichannel detector allows recording directly the entire transient spectra, independently of the shot-to-shot fluctuations and possible long-term drifts of the electron source.

All the measurements were made in a FSOFC with a 5 mm optical path collinear to the electron pulse propagation. Under the experimental conditions, the time resolution is mainly determined by the electron pulse duration and the velocity mismatch between the electron pulse and the slower visible probe pulse during their propagation inside the cell. Fitting the rise of the absorption signal of the solvated electron, a species that is formed on the femtosecond scale, by a step function convoluted with a Gaussian cross-correlation revealed an apparatus function of full width at half-maximum of 12 ps. More details on the optical configuration and the data acquisition can be found in ref 15.

The solutions containing nitric acid at high concentration and pure water were studied under identical experimental conditions. Particular attention was paid for a constant dose per pulse. Transient spectra were recorded on the pico- to low nanosecond scale; the kinetics were traced after data acquisition at selected wavelengths. The temporal evolution of each sample under investigation was scanned in the order of 30 times with a single point averaging of 10 for each delay step. The measurements were performed at 22.5 °C, the room temperature during the picosecond pulse radiolysis experiments. The nitric acid was purchased from Sigma-Aldrich. Water for dilution was purified by passage through a Millipore purification system.

RESULTS AND DISCUSSION

The kinetics at 640 nm recorded directly after the electron pulse are presented in Figure 1 for each studied system. For the

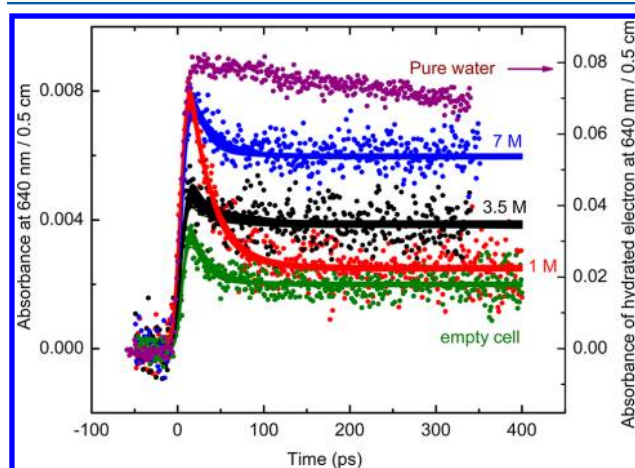


Figure 1. Kinetics at 640 nm recorded directly after the electron pulse for pure water (right axis), empty FSOFC, and solutions containing 1, 3.5, and 7 M solutions of HNO_3 ; optical path = 0.5 cm. The fits of data are performed by Bayesian data analysis using a multiexponential equation convoluted with a Gaussian instrument response function. The thickness of the lines represents the model uncertainty.

solutions containing nitric acid, the amplitude of the signals of the transient absorption is more than ten times lower than in pure water. The measurements in pure water and in concentrated acid solutions are performed in the same FSOFC of 0.5 cm and at the identical position relative to the accelerator exit to ensure a constant dose for the different solutions under investigation. The signal in pure water corresponds to the absorption of the hydrated electron and is used for dosimetry. As we reported recently,¹⁶ the empty FSOFC presents under irradiation also a transient absorption

band in the visible region. This contribution of the empty FSOFC is of the same order of magnitude as those obtained for nitric acid solutions and has therefore to be subtracted from the transient signals of the samples. Moreover, for highly concentrated aqueous solutions, it is important to note that the dose given by dosimetry in pure water should be corrected by the factor F as follows:¹⁷

$$F = d_{\text{sol}}(Z_{\text{NO}_3}p/A_{\text{HNO}_3} + Z_{\text{water}}(100 - p)/A_{\text{water}}) / (Z_{\text{water}}100/A_{\text{water}})^{-1} \quad (13)$$

where d_{sol} is the density of the solution, Z is the number of electrons, A is the mass number, and p is the weight fraction of the solute. The dose absorbed by a solution is

$$D_{\text{sol}} = FD_{\text{water}} \quad (14)$$

The value of F is 1.02, 1.1, and 1.18 for the solutions containing 1, 3.5, and 7 M nitric acid, respectively. The experimental kinetics obtained for the three samples and the empty FSOFC are fitted by a linear superposition of monoexponential functions convolved with a Gaussian instrumental response function (with a full width at half-maximum of 12 ± 2 ps) (Figure 1, solid lines). The uncertainties on the fitting curves are obtained by Bayesian data analysis.^{18,19} A Monte Carlo sample of representative curves for each kinetics trace is used for the subtraction of the transient absorption induced in the windows of the FSOFC and the normalization of the dose. After these two corrections, the kinetics at 640 nm are reported in Figure 2 showing only the absorption of NO_3^\bullet radical formed by the picosecond electron pulse.

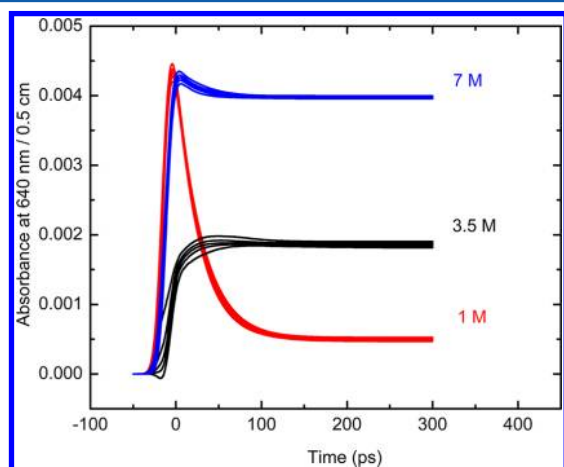


Figure 2. Kinetic recorded at 640 nm in pure water and 1, 3.5, and 7 M solutions of HNO_3 after subtraction of the empty cell contribution and after dose correction by factor F (see Table 1). Same conditions as in Figure 1.

In 1 M nitric acid solution, we observe a fast decay at very short time, which is due to the decay of the solvated electron, and a plateau that is almost stable up to around 350 ps. For the solution containing 3.5 M nitric acid, we observe only the formation of species absorbing at 640 nm, reaching a plateau after the electron pulse. In the case of the 7 M solution, a small decay is also observed at very short time, which can be due to the error of procedure of the empty cell signal subtraction and also the relative low value of S/N. However, this part of the transient absorption represents less than 5% of the amplitude of

the signal. As in the case of the 3.5 M solution, the signal reaches also a plateau. For a given absorbed dose, the amplitude of the signal reported for 7 M nitric acid is more than two times higher than for 3.5 M (Figure 2).

Figure 3 presents the absorption spectrum recorded in 7 M of nitric acid solution 200 ps after the electron pulse. The

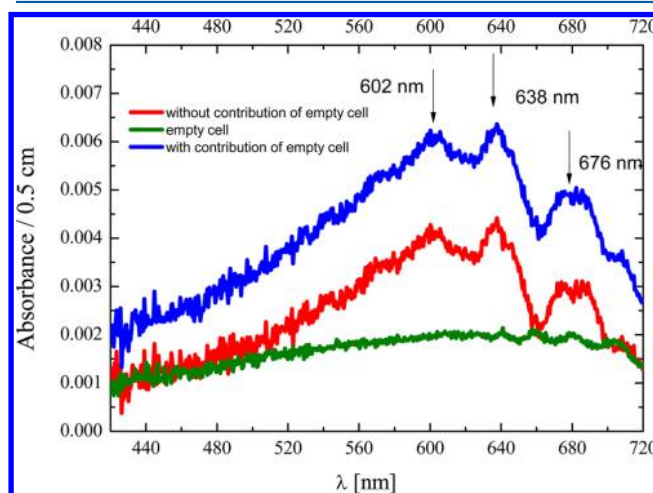


Figure 3. Transient absorption spectra recorded directly after the picosecond electron pulse (blue) in 7 M HNO_3 and (green) in the empty FSOFC. (red) The contribution of transient absorption issued from the windows of FSOFC is subtracted.

transient absorption spectrum recorded after the electron pulse shows three maxima at 602, 638, and 676 nm, which bears witness for the formation of the nitrate radical NO_3^\bullet .²⁰ These three maxima are in agreement with the spectrum of nitrate radical reported elsewhere in the literature.⁸ Other transient species resulting from the radiolysis of nitric acid do not contribute to the absorbance at 640 nm.²¹ For example, the $\text{NO}_3^{2-\bullet}$ radical absorbs in the UV region with a maximum at 250 nm.²² The radical $\text{H}_2\text{NO}_3^\bullet$ arising from the protonation of the $\text{NO}_3^{2-\bullet}$ is assumed neither to contribute to the absorption at 640 nm; however, no data concerning $\text{H}_2\text{NO}_3^\bullet$ is available. Therefore, the kinetics reported in Figure 2 corresponds to the formation of NO_3^\bullet radicals, except the fast decay at short time observed in the case of 1 M nitric acid corresponding to the decay of solvated electron. The decay of the solvated electron is attributed to the reaction 1 and the reaction with H^+ by considering the following kinetics:

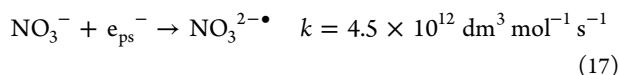
$$[e_s^-]_t = [e_s^-]_{t=0} \exp(-k_{\text{obs}}t) \quad (15)$$

with

$$k_{\text{obs}} = k_{\text{H}^+}[\text{H}^+] + k_2[\text{NO}_3^-] \quad (16)$$

By fitting the pseudo first order decay of solvated electron in 1 M nitric acid solution, k_{obs} was determined. Its value is $3.3 \times 10^{10} \text{ s}^{-1}$. In fact, the values of k_{H^+} and k_2 are known to be 2.3×10^{10} and $9.7 \times 10^9 \text{ M}^{-1} \text{ s}^{-1}$, respectively. By considering the 1 M HNO_3 solution, k_{obs} should be $3.27 \times 10^{10} \text{ s}^{-1}$, which is in good agreement with the value obtained from the exponential fit of the kinetics. The half time decay of solvated electron in 1 M HNO_3 solution is therefore 21 ps, which indicates that the solvated electron is scavenged directly after its formation. The decay of solvated electron is not observed in the case of the solutions containing 3.5 and 7 M nitric acid. In fact, by considering the same reactions, the half time of the solvated

electron in these solutions is 6 and 3 ps, respectively. Moreover, it is known that the presolvated electron is also efficiently scavenged by NO_3^- :²³



For these reasons, for the solution of 3.5 and 7 M nitric acid, the signal of the solvated electron cannot be observed with our time resolution, and we observe only the signal due to the formation of NO_3^\bullet (Figures 1 and 2). The reaction 17 is too fast to be observed directly with our experimental setup. The value 4.5×10^{12} is an estimation reported in the literature. According to our observations, we can just claim that the rate constant of this reaction is larger than $2 \times 10^{12} \text{ M}^{-1} \text{ s}^{-1}$. In fact, in 7 M acid nitric solution, the amplitude of the kinetics observed at 780 nm (not reported here), where only hydrated electron absorbs, is lower than 2% of the amplitude of the kinetics in pure water. This implies that nitrate ions scavenge very efficiently the precursor of the solvated electron.

Knowing the dose absorbed by the solutions as well as the molar absorption coefficient of the nitrate radical NO_3^\bullet at 640 nm, the yield of NO_3^\bullet formation can be calculated from the value of the kinetics after full decay of the solvated electron. Taking into account the molar absorption coefficient, $\epsilon_{640 \text{ nm}} = 1300 \pm 100 \text{ M}^{-1} \text{ cm}^{-1}$,⁸ the experimental yield of NO_3^\bullet is found to be $0.36 \times 10^{-7} \text{ mol J}^{-1}$, $1.33 \times 10^{-7} \text{ mol J}^{-1}$, and $2.85 \times 10^{-7} \text{ mol J}^{-1}$ for 1, 3.5, and 7 M nitric acid solution, respectively. It is interesting to compare these yields with those reported in the literature. The first pulse radiolysis study of nitric acid proposed that the direct effect forms NO_3^\bullet ; however, it was reported that the radical is not the primary species because, under certain conditions, the kinetic curves give indications of a rise time, though this could not be completely resolved.²⁴ The author suggested that the radical is formed through the reaction 8 and the following:²⁵



On the basis of a radiolysis study with a $2.5 \mu\text{s}$ long electron pulse, the dependence of the NO_3^\bullet yield on HNO_3 concentration was reported to be around $13 \times 10^{-7} \text{ mol J}^{-1}$,²⁶ but this high value was due to the low value of the extinction coefficient ($300 \text{ M}^{-1} \text{ cm}^{-1}$) used for NO_3^\bullet . Using the same extinction coefficient as in the present work ($1300 \text{ M}^{-1} \text{ cm}^{-1}$), the experimental yield of direct formation of NO_3^\bullet for 6 M nitric acid solution becomes $3 \times 10^{-7} \text{ mol J}^{-1}$. This yield is slightly higher than our value on the picosecond range. The reason is that, at the microsecond time scale, reaction 7, the indirect NO_3^\bullet formation can be also involved. In fact, a few percent of nitric acid is not dissociated and can scavenge the OH^\bullet radical in the spurs. In the last pulse radiolysis measurements, a nanosecond electron pulse was used with a 10 cm optical path for measuring the formation of NO_3^\bullet and the fast component of the signal observed for 3 and 6 M nitric acid solution was attributed to the direct formation of NO_3^\bullet with an experimental yield of $0.94 \times 10^{-7} \text{ mol J}^{-1}$ and $1.5 \times 10^{-7} \text{ mol J}^{-1}$, respectively.⁸ These yields are lower than our values $1.33 \times 10^{-7} \text{ mol J}^{-1}$ and $2.85 \times 10^{-7} \text{ mol J}^{-1}$ on the picosecond range for almost the same solutions. It was reported that NO_3^\bullet decays by a first order process with rate constant of $9.5 \times 10^2 \text{ s}^{-1}$ (which is too low to have any effect at the picosecond range).²⁰ Therefore, the difference between the values of the yields cannot be due to the decay of NO_3^\bullet . To be sure, we measured also the kinetics at 640 nm at longer time.

With a similar procedure as for Figure 2, the signals measured at 640 nm are corrected by the contribution of the empty cell, and the absorption curves only due to the NO_3^\bullet radical are deduced (Figure 4). As reported in the Figure 4, we did not

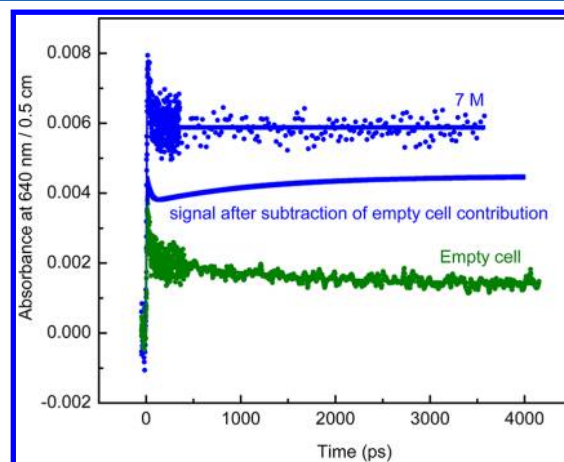


Figure 4. Kinetics recorded at 640 nm (green) in the empty cell and (blue) the cell containing 7 M solution of HNO_3 . The solid line is after subtraction of the empty FSOFC contribution. Same conditions as those in Figure 1.

observe any decay of the signal, at least during the first 4 ns. We even find a slight increase of the absorbance after the picosecond pulse that we will discuss below. Katsumura et al.⁸ considered that their results can be well fitted with the initial yield of ionization of NO_3^- equal to $4.9 \times 10^{-7} \text{ mol J}^{-1}$ or by considering the hole trapping with the yield of $\text{H}_2\text{O}^{\bullet+}$ equal to $5.1 \times 10^{-7} \text{ mol J}^{-1}$ and with a rate constant of reaction 11 ten times larger than that of reaction 12. They concluded that their results do not exclude the dry hole trapping mechanism provided it is not the dominant process.

We estimate here the dose absorbed directly by NO_3^- by taking into account the electron density fraction, $f_s = 0.06, 0.19$, and 0.35 , for the solution of 1, 3.5, and 7 M nitric acid, respectively. Taking into account the dose absorbed by the solute and considering only the direct ionization of NO_3^- as the mechanism of NO_3^\bullet formation (reaction 10), we find the value of the direct ionization yield reported in Table 1. Contrary to the expected results, we observe that the value of the NO_3^\bullet formation yield within the pulse is increasing with the concentration of NO_3^- . The increase of the yield with the initial concentration of nitric acid is not negligible. Moreover, the values are rather high ($8.1 \pm 0.5 \times 10^{-7} \text{ mol J}^{-1}$) compared to the usual yield of ionization on the picosecond range, observed, for example, for water or for halide anions (around $4.2 \times 10^{-7} \text{ mol J}^{-1}$ and $4.8 \times 10^{-7} \text{ mol J}^{-1}$, respectively¹²). That means clearly that the formation of NO_3^\bullet radical is not only due to the direct ionization of nitrate but also, we must consider, another ultrafast path that occurs within the electron pulse and that is concentration dependent. Therefore, we consider the dry hole trapping mechanism in the formation of NO_3^\bullet radical. Such a hole trapping for highly concentrated anions has been recently demonstrated clearly by picosecond pulse radiolysis measurements in the case of Cl^- and Br^- concentrated solutions.¹³ Recently, Shkrob et al. considered that, in imidazolium ionic liquid, NO_3^\bullet is also formed by hole scavenging.²⁷ For this scenario, the experimental yield can be expressed by the following relationship:

Table 1

solution (M)	[H ₂ O]/[NO ₃ [−]]	<i>F</i> ^a	observed <i>t</i> _{1/2} ^b (ps)	calculated <i>t</i> _{1/2} ^c (ps)	<i>A</i> _{<i>t</i>} =200 ps 10 ^{−3d}	<i>G</i> _{exp} (NO ₃ [•]) ^e 10 ^{−7} mol J ^{−1}	<i>f</i> _s ^f	<i>G</i> _{exp} (NO ₃ [•])/ <i>f</i> _s ^g 10 ^{−7} mol J ^{−1}
1	53.2	1.02	21	21	0.50	0.36	0.06	6 ± 0.5
3.5	14	1.1	<5	6.5	1.85	1.33	0.19	7 ± 0.5
7	5.85	1.18	<5	3	3.96	2.85	0.35	8.1 ± 0.5

^aFactor of dose absorption compared with the dose in pure water. ^bDecay half time deduced from the observed transient absorption. ^cHalf time of solvated electron calculated from the eq 15. ^dExperimental absorbance (*l* = 0.5 cm) observed at 640 nm, 200 ps after the electron pulse, corrected by the dose absorption factor *F* (the dose is 21.4 Gy per pulse), and after subtraction of the absorption due to the empty cell recorded under the same experimental conditions. ^eSeduced experimental radiolytic yield of NO₃[•] formation after the picosecond electron pulse. ^f*f*_s is the electron fraction of HNO₃. ^gExpected yield taking into account the dose absorbed directly by NO₃[−] and considering only the direct ionization process as the mechanism of NO₃[•] formation.

$$G_{\text{exp}} = f_s G_{\text{dir}} + f_w \alpha G_{\text{indirect}} \quad (19)$$

where *G*_{dir} is the yield of direct ionization of NO₃[−], *f*_w is the fraction of water electron density, and *α* is the fraction of hole oxidizing NO₃[−]. The H₂O^{•+} radical cation is a highly oxidizing species, and at high solute concentration, reaction 11 competes with the proton transfer of reaction between H₂O^{•+} and H₂O, which occurs in pure water approximately in 10 fs.^{28,29} If the proton transfer is ultrafast in pure water, for the solution containing 7 M nitric acid (total 14 M cations and anions), reaction 11 can compete with reaction 12 due to the lower probability of the presence of a water molecule close to the H₂O^{•+} cation compared to pure water. In such solution, the water concentration is only 41 M, and each water molecule is related to a cation or an anion. Therefore, a direct charge transfer from NO₃[−] to H₂O^{•+} could be proposed. Without considering such a reaction, it is not obvious to explain the high yield of NO₃[•] radical formation within the picosecond electron pulse. Moreover, as it is reported in Table 1, the efficiency of hole trapping is concentration dependent. Assuming that the yield of the direct effect by ionization, *G*_{dir}, of NO₃[−] (or HNO₃) is around 4.5 × 10^{−7} mol J^{−1} and considering that the experimental yield of NO₃[•] radical formed just after the pulse, we find that the yield of hole trapping (*αG*_{indirect}) is 0.1 × 10^{−7} mol J^{−1}, 0.59 × 10^{−7} mol J^{−1}, and 1.96 × 10^{−7} mol J^{−1} for the solutions containing 1, 3.5, and 7 M nitric acid, respectively. The yield of H₂O^{•+} is unknown but can be estimated with the yield of OH[•] radical on the picosecond range. On the basis of the corresponding value of 4.85 × 10^{−7} mol J^{−1} that we published recently,³⁰ we find an *α* value equal to 2%, 12% and 40% for the solutions containing 1, 3.5, and 7 M nitric acid, respectively. The proton transfer reaction 12 is an efficient pathway even for 7 M solution. By considering the competition between reaction 11 and the proton transfer reaction with water (reaction 12), a rough estimation of the value of *k*₁₂ gives 2 × 10¹³ M^{−1} s^{−1}, which is close to the rate constant of the ion–molecule reaction known in the gas phase (8 × 10¹² M^{−1} s^{−1}). It is important to note that the rate constant of the proton reaction can be modified in highly acidic solution, and our rough estimation is based on the value of *k*₁₂ known in pure water.

Eventually, it is important to note that we observe a slight increase of the transient absorption observed at 640 nm after the pulse on the nanosecond scale (Figure 4). The direct effect and hole trapping occurs only within the electron pulse. Therefore, another mechanism should be considered to explain the supplementary amount of NO₃[•] radical formation. At first, let us consider the reaction of OH[•] radical with undissociated nitric acid through reaction 7. If we consider the same value of the rate constant of reaction³¹ and an equilibrium constant for a

7 M nitric acid solution (*K* = 12 M^{−1}),^{32,33} the reaction between OH[•] and undissociated nitric acid can occur partially, and the slight increase of the signal within the first 4 ns could be to that reaction (Figure 4). Nevertheless, we cannot exclude a very low contribution of the reaction 18. In fact, the oxygen atom is scavenged by NO₃[−] very quickly to form O₂, but a small amount of oxygen atom could recombine with NO₂[•] to form the radical NO₃[•] in the spurs. However, we can surely state that this recombination is negligible in our conditions. In fact, it was reported that the yield of O₂ is increasing by increasing the concentration of NO₃[−] in solution,³⁴ which is in favor of the reaction between oxygen atom and NO₃[−].

CONCLUSIONS

A careful analysis of the kinetics observed on the picosecond range in highly concentrated nitric acid solutions shows that the direct effect of irradiation is a major process in solutions with concentrations higher than 1 M. We observed that the radical NO₃[•] is formed just after the pulse, showing clearly that the mechanism of its formation by direct effect is not through reactions 8 or 9 but is formed directly through reaction 10. Moreover, the yield of this radical is too high to consider only reaction 10 as responsible for its formation. We have found strong evidence that the hole is also trapped by nitrate to form the same radical through reaction 11. This observation is important for the estimation of the yield of OH[•] in such conditions. In fact, not all of the holes are converted to OH[•] as hole trapping is not negligible. Finally, we observed that this radical is rather stable during the first 4 ns and that it is not involved in the spur reactions at short time. The amount of the NO₃[•] radical, after the picosecond pulse, is even slightly increased due to reaction 7. The results of this study could be implemented in the simulation codes usually used for modeling the radiolysis of nitric acid and its application to radiation chemistry of nuclear waste and reprocessing treatments in nitric acid medium.

AUTHOR INFORMATION

Corresponding Author

*E-mail: mehran.mostafavi@u-psud.fr.

Notes

The authors declare no competing financial interest.

ACKNOWLEDGMENTS

We thank RTRA, Tringle de la Physique (France), who supported ELYSE team financially to improve the experimental setup.

■ REFERENCES

- (1) Polevoi, P.; Ross, A. B. *Radiat. Phys. Chem.* **1987**, *29*, 161–174.
- (2) Wolff, R. K.; Bronskill, M. J.; Hunt, J. W. *J. Phys. Chem.* **1970**, *53*, 4211–4216.
- (3) Wayne, R. P.; Barnes, I.; Biggs, P.; Burrows, J. P.; Canosa-Mas, C. E.; Hjorth, J.; Le Bras, G.; Moortgat, G. K.; Perner, D.; Poulet, G.; et al. *Atmos. Environ.* **1991**, *25*, 1–203.
- (4) Katsumura, Y. Application of Radiation Chemistry to Nuclear Technology. In *Charged Particle and Photon Interaction with Matter, Chemical, Physicochemical, and Biological Consequences with Applications*; Mozumder, A., Hatano, Y., Eds.; Marcel Dekker: New York, 2004; pp 697–727.
- (5) Buxton, G.; Greenstock, G. L.; Hermann, W. P.; Ross, A. B. *J. Phys. Chem. Ref. Data* **1988**, *17*, 513–886.
- (6) Grätzel, M.; Henglein, A.; Lilie, J.; Beck, G. *Ber. Bunsenges. Phys. Chem.* **1970**, *74*, 292–298.
- (7) Logager, T.; Sehested, K.; Holcman, J. *J. Phys. Chem.* **1993**, *97*, 6664–6669.
- (8) Katsumura, Y.; Jiang, P. Y.; Nagaishi, R.; Ishigure, K.; Yoshida, Y. *J. Phys. Chem.* **1991**, *95*, 4435–4439.
- (9) Daniels, M. *Adv. Chem. Ser.* **1968**, *82*, 153–163.
- (10) Jiang, P.-Y.; Nagaishi, R.; Yotsuyanagi, T.; Katsumura, Y.; Ishigure, K. *J. Chem. Soc., Faraday Trans.* **1994**, *90*, 93–95.
- (11) Marsalek, O.; Elles, C. G.; Pieniazek, P. A.; Pluhařová, E.; VandeVondele, J.; Bradforth, S. E.; Jungwirth, P. *J. Chem. Phys.* **2011**, *135*.
- (12) Balcerzyk, A.; LaVerne, J. A.; Mostafavi, M. *J. Phys. Chem.* **2011**, *115* (17), 4326–4333.
- (13) Balcerzyk, A.; Schmidhammer, U.; El Omar, A. K.; Jeunesse, P.; Larbre, J. P.; Mostafavi, M. *J. Phys. Chem.* **2011**, *115* (33), 9151–9159.
- (14) Belloni, J.; Crowell, R. A.; Katsumura, Y.; Lin, M.; Marignier, J. – L.; Mostafavi, M.; Muroya, Y.; Akinori, S.; Tagawa, S.; Yoshida, Y.; et al. In *Recent Trends in Radiation Chemistry*; Wishart, J. F., Rao, B. S. M., Eds.; World Scientific: Hackensack, NJ, 2010; pp 121–160.
- (15) Schmidhammer, U.; Pernot, P.; De Waele, V.; Jeunesse, P.; Demarque, A.; Murata, S.; Mostafavi, M. *J. Phys. Chem. A* **2010**, *114*, 12042–12051.
- (16) Schmidhammer, U.; El Omar, A. K.; Balcerzyk, A.; Mostafavi, M. *Radiat. Phys. Chem.* **2012**, DOI: [dx.doi.org/10.1016/j.radphyschem.2012.05.020](https://doi.org/10.1016/j.radphyschem.2012.05.020).
- (17) Pucheault, J.; Ferradini, C.; Julien, R.; Deysine, A.; Gilles, L.; Moreau, M. *J. Phys. Chem.* **1978**, *83*, 330–336.
- (18) Soroushian, B.; Lampre, I.; Bonin, J.; Pernot, P.; Pommeret, S.; Mostafavi, M. *J. Phys. Chem. A* **2006**, *110* (5), 1705–1717.
- (19) Bonin, J.; Lampre, I.; Pernot, P.; Mostafavi, M. *J. Phys. Chem. A* **2007**, *111* (23), 4902–4913.
- (20) Dogliotti, L.; Hayon, E. *J. Phys. Chem.* **1967**, *71* (12), 3802–3808.
- (21) Logager, T.; Sehested, K.; Holcman, J. *Radiat. Phys. Chem.* **1993**, *41* (3), 539–543.
- (22) Grätzel, M.; Henglein, A.; Taniguchi, S. *Ber. Bunsenges. Phys. Chem.* **1970**, *74* (3), 292–298.
- (23) Pimblott, S. M.; LaVerne, J. A. *J. Phys. Chem. A* **1998**, *102*, 2967–2975.
- (24) Daniels, M. *J. Phys. Chem.* **1966**, *70*, 3022–3024.
- (25) Daniels, M. *J. Phys. Chem.* **1969**, *73*, 3710–3717.
- (26) Kozłowska-Milner, E.; Broszkiewicz, R. *Radiat. Phys. Chem.* **1978**, *11*, 253–260.
- (27) Shkrob, I. A.; Marin, T. W.; Chemerisov, S. D.; Wishart, J. F. *J. Phys. Chem. B* **2011**, *115*, 3872–3888.
- (28) De Waele, V.; Lampre, I.; Mostafavi, M. In *Charged Particle and Photon Interactions with Matter*; Hatano, Y.; Katsumura, Y.; Mozumder, A., Eds.; CRC Press, Boca Raton, FL, 2011; pp 289–324.
- (29) Garrett, B. C.; Dixon, D. A.; Camaioni, D. M.; Chipman, D. M.; Johnson, M. A.; Jonah, C. D.; Kimmel, G. A.; Miller, J. H.; Rescigno, T. N.; Rossky, P. J.; et al. Role of water in electron-initiated processes and radical chemistry: Issues and scientific advances. *Chem. Rev.* **2005**, *105*, 355–389.
- (30) El Omar, A. K.; Schmidhammer, U.; Jeunesse, P.; Larbre, J.-P.; Lin, M.; Muroya, Y.; Katsumura, Y.; Pernot, P.; Mostafavi, M. *J. Phys. Chem. A* **2011**, *115* (44), 12212–12216.
- (31) In the first article (ref 7), the value of the rate constant for reaction 7 was reported to be $1.4 \times 10^8 \text{ mol}^{-1} \text{ L s}^{-1}$. We checked the data and found that this value should be corrected to $5.3 \times 10^7 \text{ mol}^{-1} \text{ L s}^{-1}$. Recently, this latter value was confirmed in the following review: Takagi, J.; Mincher, B. J.; Yamaguchi, M.; Katsumura, Y. In *Charged Particles and Photon Interaction with Matter, Recent Advances, Applications and Interfaces*; Hatano, Y., Katsumura, Y., Mozumder, A., Eds.; Radiation Chemistry in Nuclear Engineering CRC Press: Boca Raton, FL, 2011; Chapter 34, pp 959–1023.
- (32) Krawetz, A. A. *A Raman Spectral Study of Equilibria in Aqueous Solutions of Nitric Acid*. Ph.D. Thesis, University of Chicago, 1955.
- (33) Ruas, A.; Pochon, P.; Simonin, J. P.; Moisy, P. *Dalton Trans.* **2010**, *39*, 10148–10153.
- (34) Nagaishi, R.; Jiang, P.-Y.; Katsumura, Y.; Ishigure, K. *J. Chem. Soc., Faraday Trans.* **1994**, *90*, 591–594.